Effect of doping of 8-hydroxyquinolinatolithium on electron transport in tris(8-hydroxyquinolinato)aluminum

Arunandan Kumar,[1,2] Ritu Srivastava,[1,a)] Priyanka Tyagi,[1] D. S. Mehta,[2] and M. N. Kamalasanan[1]

[1]*Center for Organic Electronics, National Physical Laboratory (Council of Scientific and Industrial Research), Dr. K.S.Krishnan Road, New Delhi 110012, India*

[2]*Instrument Design and Development Center, Indian Institute of Technology Delhi, New Delhi 110016, India*

(Received 4 December 2010; accepted 29 April 2011; published online 13 June 2011)

Effect of doping of 8-hydroxyquinolinatolithium (Liq) on the electron transport properties of tris(8-hydroxyquinolinato)aluminum (Alq_3) has been investigated as a function of temperature and doping concentration by fabricating electron only devices. It has been observed that current density in the devices increases with the doping of Liq up to a doping concentration of 33 wt. % and then decreases. Current density-voltage (*J-V*) characteristics of 0, 15, and 33 wt. % Liq doped Alq_3 devices were found to be bulk limited and analyzed on the basis of trap charge limited conduction model. The *J-V* characteristics of 50 and 100 wt. % Liq doped Alq_3 devices were found to be injection limited and were analyzed using the Fowler-Nordheim model. The increase in current density with doping up to 33 wt. % was found to be due to an increase in electron mobility upon doping, whereas the decrease in current density above 33 wt. % was due to the switching of transport mechanism from bulk limited to injection limited type due to an increase in barrier height. Electron mobility and variance of energy distribution have been measured by using transient electroluminescence technique to support our analysis. Electron mobility for pure Alq_3 was found to be 1×10^{-6} cm^2/V s, which increased to 3×10^{-5} cm^2/V s upon doping with 33 wt. % Liq. The measured values of variance were 95, 87.5, 80, 72, and 65 meV for 0, 15, 33, 50, and 100 wt. % Liq doped Alq_3 respectively. The increase in electron mobility upon doping has been attributed to a decrease in energetic disorder upon doping as evidenced by the decrease in variance. The increase in barrier height for the higher doping concentration was due to the disorder related correction $\sigma^2/2kT$ in the barrier height, which decreases with the increase in doping concentration.
© *2011 American Institute of Physics*. [doi:10.1063/1.3596523]

I. INTRODUCTION

Doping of organic semiconductors was first studied in the 1960s,[1] however they have been extensively studied only after their use in enhancing the carrier injection and transport properties in optoelectronic devices,[2–15] such as organic light-emitting diodes (OLEDs) and organic solar cells (OSCs). p-type doping of organic semiconductors has been studied by using a series of techniques such as ultraviolet photoelectron spectroscopy (UPS), x-ray photoelectron spectroscopy (XPS), and low temperature conductivity measurements.[16–24] As a result, p-type doping has been explained with a simple picture of doping where holes are generated in the transport level by thermal excitation of electrons to a well defined acceptor level provided by the dopant.[25] 2,3,5,6-tetrafluoro-7,7',8,8'-tetracyanoquinodimethane (F_4-TCNQ) has become a vital p-type dopant[16–24] for hole transport and injecting materials in organic light-emitting diodes.

Despite the extensive studies on p-type doping, n-type doping of organic semiconductors still remains a challenge. To create a free negative carrier in an organic semiconductor, a donor molecule is required whose highest occupied molecular orbital (HOMO) value should match with the lowest unoccupied molecular orbital (LUMO) of the host molecule. Systematic studies of n-type doping have been performed on materials with low-lying LUMO levels, that is, high electron affinity. Reasonable increases in conductivity have been achieved in naphthalenetetracarboxylic dianhydride (NTCDA) using the dopant bis(ethylenedithio)tetrathiafulvalene (BEDT-TTF).[9] The common electron transporting molecules used in OLEDs, however, have LUMO value around 3 eV which limits the choice of donor molecules for this application. Further, organic molecules with HOMO around 3 eV are highly unstable in air. Alkali metals like Li and Cs and their oxides are also used for n-type doping of organic electron transport materials[10–12] and were found useful in many instances. But this type of doping has many serious problems, like damage to underlying organic layers due to high evaporation temperatures. Furthermore, they have also been reported as luminescence quenchers,[26] which act to reduce the lifetime and stability of devices. Hence, there is a need for molecular dopants for enhancement of electron transporting properties in OLED applications. Recently 8-hydroxyquinolinatolithium (Liq) has been used as a dopant in electron transporting molecules Batho phenanthroline (Bphen) and tris(8-hydroxyquinolinato) aluminum (Alq_3).[27–29] But the reason for the enhanced electron transport property of these molecules was not well understood, especially the requirement of high doping concentrations (around

[a)]Author to whom correspondence should be addressed. Electronic mail: ritu@mail.nplindia.org.

 © 2011 American Institute of Physics

Pictiva EX2004
Samsung v Pictiva
IPR2026-00129

30%) in these molecular systems. To shed light on the physical process behind the doping, we have selected the Liq doped Alq_3 system to carry out electron transport studies. Since Bphen has very low glass transition temperature (~75°C), which causes issues related to device lifetimes, Alq_3 has been chosen in its place. For electron transport studies, we have fabricated electron only devices with device structure Al/Organic/Al and studied the effect of doping concentration of Liq on current density-voltage (*J-V*) characteristics of these devices. Furthermore, electron mobilities have been measured in the doped Alq_3 films by the transient electroluminescence technique. These measurements have been used to explain the enhanced electron mobilities in Liq doped Alq_3 films.

II. EXPERIMENTAL

Electron only devices were fabricated onto glass substrates, which were cleaned using de-ionized water, acetone, trichloroethylene and isopropyl alcohol in sequence for 20 min each using an ultrasonic bath and then dried in vacuum. The devices were fabricated in a sandwich structure, with a vacuum evaporated active organic layer sandwiched between two vacuum evaporated aluminum electrodes. The active organic layer was pure Alq_3 and Liq doped Alq_3. Doped Alq_3 films were deposited by co evaporation. Thicknesses of pure and doped Alq_3 were 100 nm. The size of the pixels was 4×4 mm^2. The organic material was deposited at the rate of 0.1 nm/s and Al was evaporated at 0.5 nm/sec. The thickness of the Al electrode was 150 nm and the whole deposition sequence were done without breaking the vacuum. The thickness of deposited films was controlled using a quartz crystal thickness monitor. The *J-V* characteristics of the devices were measured under vacuum using a Keithley 2400 source measure unit and a homemade liquid nitrogen cryostat. The injection properties of organic on metal and metal on organic were also checked by reversing the biasing and were found to be similar and within experimental error. The thicknesses of the organic layers were reconfirmed by ellipsometric methods. The active area was measured by using an optical microscope with a traveling xy stage to confirm x and y dimensions.

For the time resolved electroluminescence (EL) measurements, the OLEDs were fabricated on indium-tin-oxide (ITO) coated glass substrates having a sheet resistance of 20 Ω/sq and a thickness of 120 nm. The substrates were patterned and cleaned using de-ionized water, acetone, trichloroethylene, and isopropyl alcohol sequentially for 20 min each using an ultrasonic bath and dried in a vacuum oven. Prior to organic film deposition ITO surface was treated with oxygen plasma for 5 min to increase ITO work function.[30,31] Organic layers were deposited onto glass substrates under high vacuum (4×10^{-6} Torr) at a deposition rate of 0.4 Å/s. Thicknesses of the deposited layers were measured *in situ* by a quartz crystal thickness monitor. OLEDs have device structure of ITO (120 nm)/*N,N'*-di-[(1-naphthalenyl)-*N,N'*-diphenyl]-(1,1' biphenyl)-4,4'-diamine (α-NPD) doped with 0.4 wt. % F_4-TCNQ (40 nm)/Liq doped Alq_3 (70 nm)/Al (120 nm). The device was transferred to a liquid nitrogen cryostat where transient electroluminescence studies were carried out at different temperatures in vacuum at about 10^{-3} Torr. The capacitance of the EL device was calculated to be about 1.5 nF. Assuming the equivalent circuit of the OLED device to be a series-connected circuit of a resistor and a capacitor, the series resistance was found to be ~80 Ω and the overall *RC* time constant of the experimental setup was estimated to be less than 0.2 μs. The equivalence circuit of the OLED device was studied using a Solartron impedance gain-phase analyzer SI 1260. The transient EL setup consists of a pulse generator, a fast photo detector (photo multiplier tube; PMT) and a fast storage oscilloscope. OLED was electrically excited by applying a fast square electrical pulse from a 15 MHz function generator HAMEG HM8131-2 with accurate repetition, rise, and decay time. To study the EL rise time at different voltages the pulses with a frequency of 1 KHz and duty of 50% were applied. The time-resolved EL response of the device was measured using the PMT detector. Along with the input pulse, the detector's output was coupled to one of the input channels of a HAMEG Analog-Digital Scope HM1507-3, where the input pulse and the output EL response of the device were recorded simultaneously. By the overlapping of the input voltage pulse and the transient EL response of device, a delay in the onset of EL was clearly seen.

III. RESULTS AND DISCUSSION

Electron only devices were fabricated by sandwiching *x* wt. % Liq doped Alq_3 (here $x = 0$, 15, 33, 50, 100) between two Al electrodes. Since the work function of Al is about 4.0 eV and the LUMO value of Alq_3 is 2.7 eV,[32] the electron injection barrier between Al and Alq_3 will be very high. However, it is observed from UPS measurements that there are large interface dipoles present between Al and Alq_3 films,[33] which reduce the barrier by about 1.0 eV and thereby the actual electron injection barrier reduces to about 0.3 eV. Similarly, the energy barrier for hole injection also increases by about 1.0 eV due to interface dipoles and the resultant barrier increases to about 2.4 eV. Therefore, hole injection is expected to be very inefficient in comparison to electron injection, and any current observed in the devices will be due to electrons flowing between two Al electrodes. Therefore, the Al/organic/Al devices can be considered as electron only devices. Thicknesses of the organic films were kept at 100 nm for all five devices. Figure 1 shows the *J-V* characteristics for all the devices at room temperature. The current density increases nonlinearly with the increase in voltage for all the devices. A current density of 1 A/m^2 was reached at 15 V for the pure Alq_3 device, whereas the same current density was reached at 8 V for Alq_3 doped with 15 wt. % Liq. The voltage required to get the same current density further reduced to 5.5 V at a higher doping ratio of 33 wt. %, indicating substantial reduction in film resistance upon doping. Higher doping concentrations (50 and 100%), however, resulted in the increase in operating voltage to 13 V and 20 V for this current density, respectively.

To investigate the conduction mechanism in Liq doped Alq_3, the *J-V* characteristics of the devices were measured at different temperatures. Figures 2(a)–(e) show the *J-V*

Pictiva EX2004
Samsung v Pictiva
IPR2026-00129

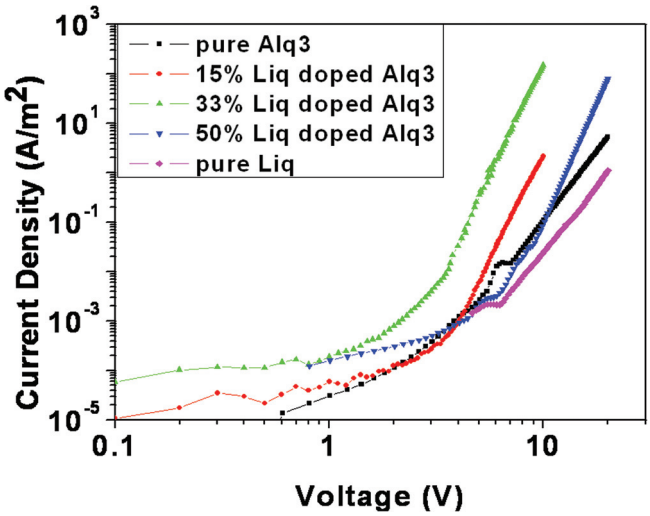

FIG. 1. (Color online) Current density-voltage characteristics of electron only devices with active layer composed with different doping ratios (0%, 15%, 33%, 50%, and 100%) of Liq in Alq_3.

characteristics of devices for 0, 15, 33, 50, and 100 wt. %, respectively, in double log scale. It can be seen that the current density is temperature dependent for devices with 0, 15, and 33 wt. % Liq doped Alq_3 as the active layer and becomes temperature independent for devices with 50 and 100 wt. % Liq doped Alq_3. This indicates a switching of conduction mechanism with the increase in doping concentration. Hence, a detailed analysis of temperature dependency of *J-V* characteristics has been carried out.

The analysis of the *J-V* characteristics of devices with 0, 15, and 33 wt. % Liq doped Alq_3 as the active layer was done on the basis of a trap charge limited conduction (TCLC) model. Figure 3 shows the *J-V* characteristics of a device with 33 wt. % Liq doped Alq_3 as the active layer at room temperature in log scale. At low applied bias voltages (below 1 V), the *J-V* characteristics show ohmic conduction, which may be due to the dominance of charge carriers generated from background doping over the injected charge carriers. As the voltage is further increased, current increases nonlinearly and log*J* versus log*V* plot shows a straight line with slope more than one, indicating a power law dependence of current density on voltage ($J \alpha V^{l+1}$). It can be seen from Fig. 2(c) that the value of the exponent l increases with the decrease in temperature. The results can be fitted into a trap charge limited conduction (TCLC) model in which the current density J can be written in the form[34–36]

$$J = q^{1-l}\mu N_v \left(\frac{2l+1}{l+1}\right)^{l+1} \left(\frac{l}{l+1}\frac{\varepsilon_s \varepsilon_0}{H_b}\right)^{l} \frac{V^{l+1}}{d^{2l+1}}, \qquad (1)$$

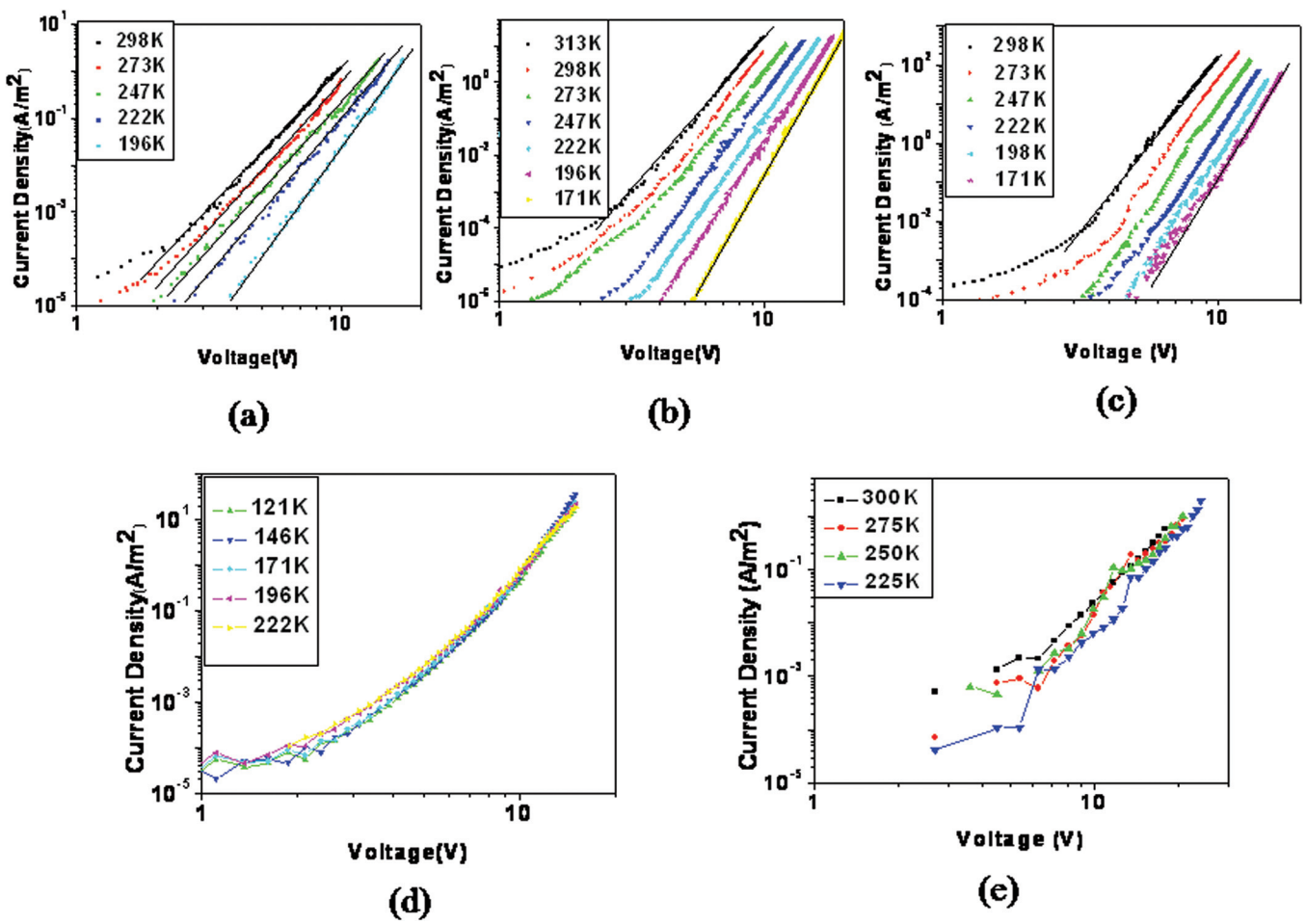

FIG. 2. (Color online) Current density-voltage characteristics of (a) 0%, (b) 15%, (c) 33%, (d) 50%, (e) 100% Liq doped Alq_3 electron only devices at different temperatures.

Pictiva EX2004
Samsung v Pictiva
IPR2026-00129

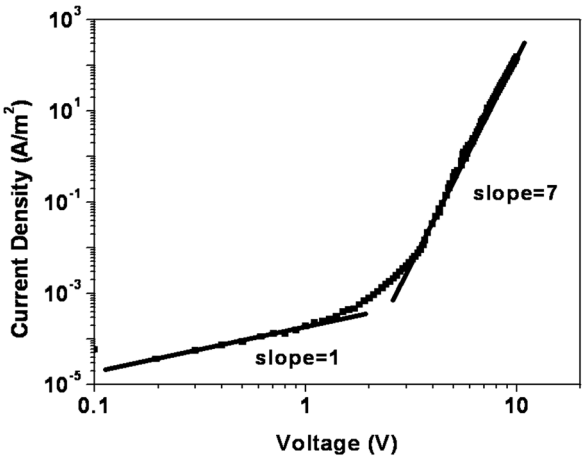

FIG. 3. Current density-voltage characteristics of 33% Liq doped Alq_3 electron only device at 298 K.

where μ is the mobility of charge carriers, N_v the molecular density, H_b the trap density, $l = \frac{T_c}{T}$ where T_c is the critical temperature given by trap energy $E_t = kT_c$, ε_s is the relative permittivity of the medium, ε_0 is the permittivity of free space, q is the charge of an electron, V is the applied voltage, and d is the thickness of the organic layer.

In the TCLC model the value of exponent l is given by T_c/T, where T_c is a constant. Therefore the value of l is expected to increase with decreasing temperatures. The value of the exponent l has been measured from the slope of J-V characteristics plotted in double logarithmic scale for all the temperatures from Figs. 2(a)–(c). To find out the critical temperature and hence the trap energy, the value of l has been plotted against 1000/T and shown in Fig. 4 for the devices with 0, 15, and 33 wt. % Liq doped Alq_3 as the active layer. The slope of these straight lines gives E_t/k, from which the value of trap energy (E_t) was calculated. The calculated values of trap energy were 0.153, 0.135, and 0.132 eV for 0, 15, and 33% Liq doped Alq_3, respectively, showing a decrease in trap energy with an increase in doping concentration. The trap energy has shown a tendency to saturate, and further increases in doping concentration did not affect the trap energy.

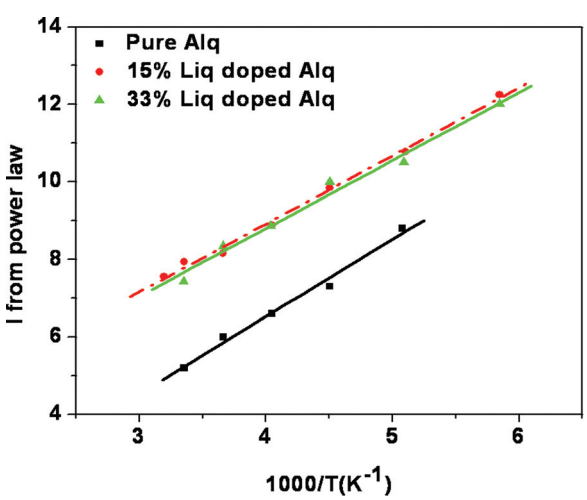

FIG. 4. (Color online) Variation of l from power law with 1000/T for 0%, 15%, and 33% Liq doped Alq_3.

The TCLC model is developed for materials that have field-independent charge carrier mobility. However, the charge carrier mobility in organic semiconductors is reported to be dependent on electric field and this dependency is of Poole-Frenkel (PF) type $\mu(F,T) = \mu_0 \exp(\beta(T)\sqrt{F})$, where parameters μ_0 and β are the zero field mobility and field lowering factor, respectively. For further detailed analysis of J-V characteristics, the field dependence of mobility has been included in Eq. (1) and experimental J-V characteristics have been fitted by adjusting the values of μ_0 and β. The used values of material parameters were $N_v = 10^{21}$ per cm^3 and $\epsilon = 3$. Figures 5 (a)–(c) shows the plot of fitted values of μ_0 and β against 1000/T. It can be seen from the figure that zero field mobility decreases, while the field lowering factor increases with the decrease in temperature. Similar behavior has been observed by many authors for different sets of materials.[34–36] The estimated values of zero field mobility at 300 K for 0, 15, and 33 wt. % Liq doped Alq_3 were 2×10^{-7}, 3×10^{-7}, 3×10^{-6} cm^2/Vs, respectively, and the values μ_0 of β were 0.0045, 0.009, and 0.009 (cm/V)[1] respectively. This indicates that the mobility ($\mu(F,T) = \mu_0 \exp(\beta(T)\sqrt{F})$) increases with an increase in doping concentration of Liq into Alq_3. Previous theoretical studies and Monte Carlo simulation results[37–41] show that for organic semiconductors the temperature dependence of zero field mobility can be written as[37–41]

$$\mu_0 = \mu(F = 0, T) = \mu_\infty \exp\left(-(2\hat{\sigma}/3)^2\right). \qquad (2)$$

Here μ_∞ is a prefactor and $\hat{\sigma} = \frac{\sigma}{kT}$, where σ is the variance of energy distribution, which has great fundamental and technological interest. This gives a measure of energetic disorder in amorphous organic semiconductors. It can be seen from Eq. (2), that log μ_0 is proportional to $1/T^2$. The value of μ_0 from the above analysis has been plotted against $1/T^2$ and from the slope of the $log\ \mu_0$ versus $1/T^2$ plot the value of σ has been calculated for 0, 15, and 33 wt. % Liq doped Alq_3. The experimentally observed values of σ were 100, 90, and 82 meV, respectively, for the above concentrations. This value of σ obtained for Alq_3 almost matches with the reported values.[34,35] From these values of σ it can be seen that as the doping concentration increases, σ decreases, indicating a decrease in energetic disorder. In order to check the effect of doping on disorder, x-ray diffraction (XRD) of undoped and doped Alq_3 films has been performed. Thicknesses of the films used for the XRD studies were 100 nm on glass substrates. Figure 5(d) shows the XRD of undoped Alq_3 and 33% wt. Liq doped Alq_3. Full width at half maximum (FWHM) of the XRD peak has decreased for doped samples. This indicates an increase in the order of the film. It has been reported that Liq is a more ordered organic semiconductor as compared to Alq_3. As more and more Liq is doped into Alq_3, the energetic disorder of the matrix has decreased. Since charge carrier mobility increases with the decrease in energetic disorder, the addition of Liq into Alq_3 leads to a decrease in energetic disorder and an increase in the charge carrier mobility, resulting in an enhancement in current density of electron only devices. However, it has been observed that the current density decreases with further increase in doping concentration.

Pictiva EX2004
Samsung v Pictiva
IPR2026-00129

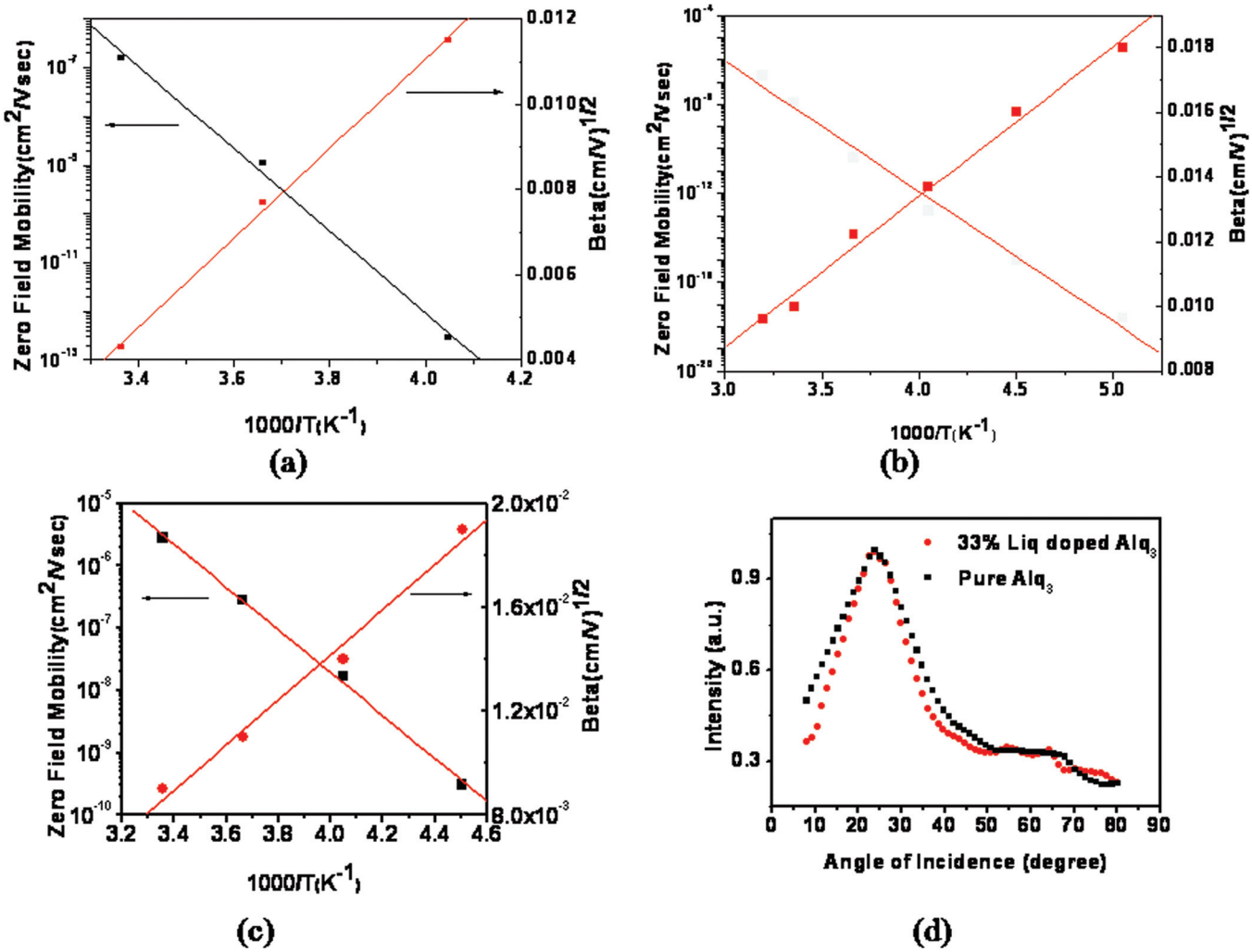

FIG. 5. (Color online) Variation of zero field mobility (μ_0) and field lowering factor (β) with $1000/T$ estimated from TCLC model with Poole-Frenkel type mobility for (a) pure Alq_3, (b) 15% Liq doped Alq_3, and (c) 33% Liq doped Alq_3 devices. (d) X-ray diffraction of pure Alq_3 and 33% Liq doped Alq_3 thin films.

To clarify this anomaly, a detailed analysis of J-V characteristics of 50 wt. % Liq doped Alq_3 and pure Liq devices has been carried out. Figures 2(d) and 2(e) show the temperature dependence of these devices. It has been seen that the J-V characteristics of a 50 wt. % Liq doped Alq_3 device is showing temperature-independent behavior above 5 V. The variation in current density with temperature is too low to account for the thermionic emission based injection mechanism. Furthermore, the value of current density is too low to account for space charge limited conduction and also the $\log J$ versus $\log V$ plot does not obey Child's law, which is the characteristic of space charge limited conduction model. The current densities in the TCLC model are highly temperature dependent and, hence, trap charge limited conduction has been ruled out. The Fowler-Nordheim (FN) tunneling mechanism is usually used to explain the injection process in the case of temperature-independent J-V characteristics. In the case of FN tunneling, the injection current density depends on the electric field (F) by the following equation:[21]

$$J = AF^2 \exp\left(-\frac{K}{F}\right) \tag{3}$$

where

$$A = \frac{q^3}{8\pi h\phi}$$
$$K = 8\pi\frac{\sqrt{2m}\phi^{3/2}}{3qh} \tag{4}$$

Here ϕ is barrier height, m the effective mass of electrons in the active material, q the charge of an electron, and h is Planck's constant. It can be seen from Eq. (3) that the plot of $\log(J/F^2)$ versus $1/F$ is a straight line for FN tunneling mechanism. Therefore, $\log(J/F^2)$ has been plotted against $1/F$ for 50 wt. % Liq doped Alq_3 and is shown in Fig. 6. The plots give straight lines in the voltage range 5–15 V. From the slope of the straight line, the barrier height has been obtained as 0.25 eV. Similar results were obtained for the pure Liq device, and the barrier height in that case was 0.30 eV. Therefore, the decrease in current density from 33 wt. % Liq doped Alq_3 device to 50 wt. % Liq doped Alq_3 device and the temperature-independent nature of the J-V characteristics can be attributed as due to the tunneling of charge carriers through the barrier, and the increased barrier height prevents carrier injection from Richardson-Schottky

Pictiva EX2004
Samsung v Pictiva
IPR2026-00129

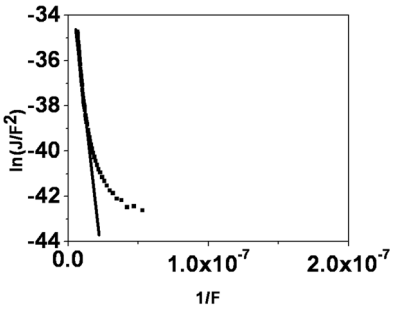

FIG. 6. Plot of $\ln(J/F^2)$ against $1/F$ for 50% Liq doped Alq_3 device.

(RS) mechanism. The further decrease in current density for the pure Liq device may be due to the increase in barrier height.

Transport studies of Liq doped Alq_3 films have shown that the current density increases upon doping upto 33 wt. % and then decreases upon further increase in the doping concentation. The increase in current density for doping concentration up to 33 wt. % has been attributed to an increase in charge carrier mobility, whereas the decrease in current density above 33 wt. % has been attributed to switching of transport mechanism from bulk limited to injection limited type due to the increase in barrier height. Furthermore, the increase in charge carrier mobility has been attributed as due to the decrease in the energetic disorder with the increase in doping concentration. To verify the increase in charge carrier mobility upon doping of Liq into Alq_3, we have measured the electron mobility and variance of energy distribution in Liq doped Alq_3 by transient electroluminescence method.

Electroluminescent devices were fabricated with a device structure of ITO (120 nm)/α-NPD doped with 0.4 wt. % F_4-TCNQ (40 nm)/Liq doped Alq_3 (70 nm)/Al. In this technique, a square voltage pulse of duration τ_{pulse} is applied to the device, maintaining a constant repetition frequency. The corresponding EL pulse was detected using a photomultiplier (PMT) tube. The delay time between the electrical and optical pulse was measured using a digital oscilloscope. This delay time is a direct measure of the transit time of the fastest carrier (electrons) toward the recombination zone. This transit time has been measured for all the devices at different electric fields and temperatures. Charge carrier mobility has been calculated from the transit time by using the expression[37]

$$\mu = \frac{d^2}{t_{tr} * V}. \tag{5}$$

Hole mobility in F_4-TCNQ doped α-NPD film is about 1×10^{-3} cm^2/Vs, which is far greater than the electron mobility in Alq_3 and, hence, the time taken by the holes to reach the F_4-TCNQ doped α-NPD/Alq_3 interface is negligible. F_4-TCNQ doped α-NPD/Alq_3 interface can be considered as a virtual collecting electrode for electrons because the movement of holes in Alq_3 will be negligible due to low hole mobility in Alq_3.[42] Hence, the delay in EL can be considered as the time taken by the electrons to travel from the electrode to the recombination zone. Therefore, the effective thickness traversed by the electrons was considered as the thickness of the Alq_3 layer for the calculation of mobility. Figure 7 shows

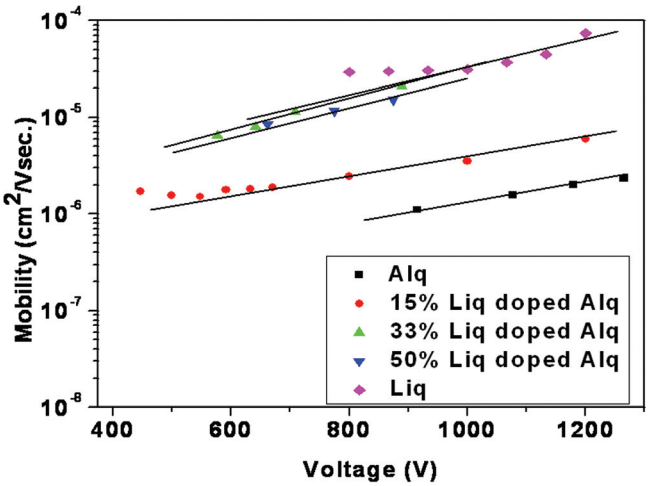

FIG. 7. (Color online) Field dependence of mobility measured using transient electroluminescence technique for 0%, 15%, 33%, 50%, and 100% Liq doped Alq_3.

the plot of mobility against square root of electric field for 0, 15, 33, 50, and 100 wt. % Liq doped Alq_3. For Alq_3, the measured value of mobility was 1×10^{-6} cm^2/Vs at a field 10^6 V/cm, which is very much closer to the value observed in many reports.[43,44] The measured mobility increases with the increase in doping concentration. For the field 10^6 V/cm, the electron mobility for 15 wt. % Liq doped Alq_3 was 3.5×10^{-6} cm^2/Vs and for 33 wt. % Liq doped Alq_3, it was 3×10^{-5} cm^2/Vs. Hence, the electron mobility has increased by about 30 times for 33 wt. % Liq doped Alq_3 compared to pure Alq_3. But further increase in doping concentration did not increase the mobility of electrons in the Liq doped Alq_3 system. To find the reason behind the increase of mobility with doping, mobility has also been measured at different temperatures. Previous theoretical studies and Monte Carlo simulation results[37–41] shows that for organic semiconductors the temperature and field dependence of mobility is given by[37–41]

$$\mu = \mu_\infty \exp\left(-\left(\frac{2}{3}\hat{\sigma}\right)^2\right) \exp\left(C\left(\hat{\sigma}^2 - \Sigma^2\right)\sqrt{F}\right). \tag{6}$$

Here C is a constant and Σ is positional disorder. For the calculation of the parameters, first the data of mobility has been extrapolated to obtain the zero field mobility. Log of zero field mobility has then been plotted against $1/T^2$. The slope and intercept of this plot gives the value of σ and μ_∞. By using the calculated values of μ_∞ and σ, positional disorder and the value of constant C have also been calculated. Table I shows the value of these parameters at different doping concentrations. It was seen that as the doping concentration increases, variance has decreased and the mobility has increased. Now after this analysis, it is possible to explain the following three important observations on Liq doped Alq_3 system: (1) Enhancement of mobility with increase in doping concentration, (2) Saturation of mobility after 33 wt. % doping, and (3) Switching of conduction mechanism from 33 wt. % Liq doped Alq_3 electron only devices to 50 wt. % Liq doped Alq_3 electron only devices.

Pictiva EX2004
Samsung v Pictiva
IPR2026-00129

TABLE I. Values of μ_∞, σ, and positional disorder for 0, 15, 33, 50, and 100% Liq doped Alq_3.

Doping concentration (wt. %)	μ_∞ (cm^2/Vs)	σ (meV)	Σ	C $(cm/V)^{1/2}$
0	4×10^{-5}	95	2.1	2.9×10^{-4}
15	4.8×10^{-5}	87.5	2.075	2.8×10^{-4}
33	5.4×10^{-5}	80	2.09	2.75×10^{-4}
50	7.6×10^{-5}	72	2.12	2.7×10^{-4}
100	7.8×10^{-5}	65	2.1	2.65×10^{-4}

It can be seen from various theoretical calculation and Monte Carlo simulation[37] that the energetic disorder is directly related to the charge carrier mobility and as energetic disorder decreases, charge carrier mobility increases. In our experiments as the doping concentration increases, the variance has decreased, which leads to the increase in charge carrier mobility. In this system it can be understood by following arguments. Liq molecule has very similar electronic properties as Alq_3 and the energy level mismatch between the two molecules is minimal. Furthermore, Liq has electron affinity of 2.8 eV and ionization energy of 5.4 eV,[45] compared to 2.7 eV and 5.4 eV respectively for Alq_3.[32] Hence, the injected electrons transfer easily from LUMO of Alq_3 to LUMO of Liq. Since Liq has been found to possess low energetic disorder, this decreases the energetic disorder of the matrix and increases the mobility. When doping concentration reached 33 wt. %, the electron mobility of Liq doped Alq_3 system reaches the value of electron mobility for Liq (Fig. 7). Hence, further increases in doping concentration does not increase the mobility and it saturates.

Now the third observation of switching of conduction mechanism can be explained by taking the variance dependence of injection barrier. It was proposed by Gartstein and Conwell[46] that the injection barrier has a energetic disorder related correction term which is experimentally observed by Marohn *et al.*,[47] this term is given by σ^2/2kT. Thus the effective injection barrier can be written as ($\Phi_b - \sigma^2$/2kT), where Φ_b is the difference between the metal work function and electron affinity of organic semiconductor. This disorder related correction makes the injected carrier density dependent on energetic disorder. Figure 8 shows the typical energy level diagram for the Al/Liq doped Alq_3 junctions for different doping concentrations of Liq. If interface dipoles are taken into account, the injection barrier at Al/Alq_3 interface is about 0.3 eV. This injection barrier decreases after including the energetic disorder related correction term. The calculated values of variance were 95, 87.5, 80, 72, and 65 meV for 0, 15, 33, 50, and 100 wt. % Liq doped Alq_3, respectively. The correction term will be 0.19, 0.15, 0.13, 0.11, and 0.08 eV for the above doping concentrations, respectively. Hence, the effective injection barrier will be 0.11, 0.15, 0.17, 0.19, and 0.22 eV for 0, 15, 33, 50, and 100 wt. % Liq doped Alq_3, respectively. This shows that as the energetic disorder decreases, the effective injection barrier at metal/organic semiconductor interface increases. In organic semiconductors the injected carrier density is dependent on the injection barrier by the equation[46,47]

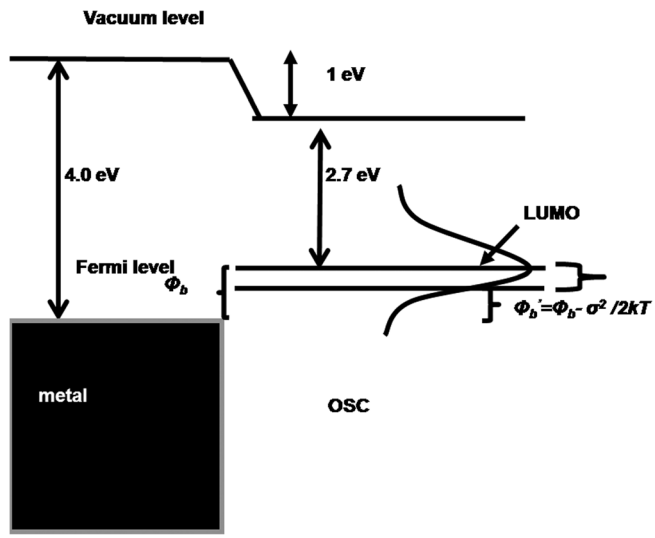

FIG. 8. Energy level diagram for Al/organic interface after taking the correction due to energetic disorder.

$$\rho = \rho_0 \exp\left(-\frac{\varphi_b}{kT}\right), \tag{7}$$

where ρ_0 is the molecular density at the metal organic interface. Therefore, as the energy barrier Φ_b increases, the injected carrier density decreases. In our experiments, the decrease in carrier density with increase in doping concentration may be due to the increase in barrier height induced by decrease in energetic disorder. This increase in barrier height with doping concentration has resulted in a decrease in injection rate, leading to injection limited conduction at higher doping ratios.

IV. CONCLUSION

Effect of doping of Liq on the electron transport in Alq_3 has been studied as a function of doping concentration. Variance of energy distribution has been found to be decreasing with the increase in doping concentration of Liq into Alq_3. Decrease in variance gives rise to the decrease in energetic disorder of Liq doped Alq_3 matrix, thus increasing the electron mobility in Alq_3 with doping of Liq. Furthermore, the energetic disorder related correction σ^2/2kT in barrier height decreases with the decrease in variance of energy distribution with doping. This causes the increase in barrier height with doping of Liq, which then resulted in a switching of conduction mechanism from bulk to injection limited type.

ACKNOWLEDGMENTS

The authors are thankful to the Director, National Physical Laboratory, New Delhi for continuous encouragement. The authors also gratefully recognize the financial support from the Department of Science and Technology (DST) and Council of Scientific and Industrial Research (CSIR) New Delhi, India for funding.

[1]For example, see M. Pope and C. E. Swenberg, *Electronic Processes in Organic Crystals and Polymers* (Oxford University Press, Oxford, UK, 1999).

Pictiva EX2004
Samsung v Pictiva
IPR2026-00129

[2]M. Pfeiffer, A. Beyer, T. Fritz, and K. Leo, Appl. Phys. Lett. **73**, 729 (1998).
[3]M. Pfeiffer, A. Beyer, T. Fritz, and K. Leo, Appl. Phys. Lett. **73**, 3202 (1998).
[4]M. Pfeiffer, T. Fritz, J. Blochwitz, A. Nollau, B. Plönnigs, A. Beyer, and K. Leo, Adv. Solid State Phys. **39**, 77 (1999).
[5]C. Ganzorig and M. Fujihira, Appl. Phys. Lett. **77**, 4211 (2000).
[6]X. Zhou, M. Pfeiffer, J. Blochwitz, A. Werner, A. Nollau, T. Fritz, and K. Leo, Appl. Phys. Lett. **78**, 410 (2001).
[7]W. Gao and A. Kahn, Appl. Phys. Lett. **79**, 4040 (2001).
[8]W. Gao and A. Kahn, Org. Electron. **3**, 53 (2002).
[9]A. Nollau, M. Pfeiffer, T. Fritz, and K. Leo, J. Appl. Phys. **87**, 4340 (2000).
[10]J. Kido, K. Nagai, and Y. Okamoto, IEEE Trans. Electron Devices **40**, 1342 (1993).
[11]J. Kido and T. Matsumoto, Appl. Phys. Lett. **73**, 2866 (1998).
[12]A. Werner, F. Li, K. Harada, M. Pfeiffer, T. Fritz, K. Leo, and S. Machill, Adv. Funct. Mater. **14**, 255 (2004).
[13]F. Li, A. Werner, M. Pfeiffer, K. Leo, and X. J. Liu, Phys. Chem. B **108**, 17076 (2004).
[14]D. Gebeyehu, B. Maennig, J. Drechsel, K. Leo, and M. Pfeiffer, Sol. Energy Mater. Sol. Cells **79**, 81 (2003).
[15]B. Maennig, J. Drechsel, D. Gebeyehu, P. Simon, F. Kozlowski, A. Werner, F. Li, S. Grundmann, S. Sonntag, M. Koch, K. Leo, M. Pfeiffer, H. Hoppe, D. Meissner, N. S. Saricifci, I. Riedel, and J. Parisi, Appl. Phys. A **79**, 1 (2004).
[16]M. Pfeiffer, A. Beyer, T. Fritz, and K. Leo, Appl. Phys. Lett. **73**, 3202 (1998).
[17]B. Maennig, M. Pfeiffer, A. Nollau, X. Zhou, K. Leo, and P. Simon, Phys. Rev. B **64**, 195208 (2001).
[18]Y. Shirota, Y. Kuwabara, and H. Inada, Appl. Phys. Lett. **65**, 807 (1994).
[19]J. S. Huang, M. Pfeiffer, A. Werner, J. Blochwitz, K. Leo, and S. Y. Liu, Appl. Phys. Lett. **80**, 139 (2002).
[20]M. Pfeiffer, T. Fritz, J. Blochwitz, A. Nollau, B. Plönnigs, A. Beyer, and K. Leo, Adv. Solid State Phys. **39**, 77 (1999).
[21]W. Gao and A. Kahn, Appl. Phys. Lett. **79**, 4040 (2001).
[22]Y. Shirota, J. Mater. Chem. **10**, 1 (2000).
[23]P. M. Borsenberger and J. J. Fitzgerald, J. Phys. Chem. **97**, 4815 (1993).
[24]R. Krause, Diploma Thesis, Technische Universität Dresden, 2005.
[25]J. Kido and T. Matsumoto, Appl. Phys. Lett. **73**, 2866 (1998).
[26]M. A. Khan, W. Xu, K. Haq, Y. Bai, F. Wei, X. Y. Jiang, Z. L. Zhang, and W. Q. Zhu, J. Phys. D **40**, 6535 (2007).
[27]P. Tyagi, R. Srivastava, A. Kumar, G. Chauhan, A. Kumar, S. S. Bawa, and M. N. Kamalasanan, Synth. Met. **160**, 1126 (2010).
[28]W. Xu, M. A. Khan, Y. Bai, X. Y. Jiang, Z. L. Zhang, and W. Q. Zhu, Curr. Appl. Phys. **9**, 732 (2009).
[29]J. W. Ma, W. Xu, X. Y. Jiang, and Z. L. Zhang, Synth. Met. **158**, 810 (2008).
[30]H. Jung and H. S. Choi, J. Electrochem. Soc. **155**, H334 (2008).
[31]Z. H. Huang, X. T. Zeng, X. Y. Sun, E. T. Kang, J. Y. H. Fuh, and L. Lu, Org. Electron. **9**, 51 (2008).
[32]R. Q. Zhang, C. S. Lee, and S. T. Lee, J. Chem. Phys. **112**, 8614 (2000).
[33]H. Ishii, K. Sugiyama, E. Ito, and K. Seki, Adv. Mater. **11**, 605 (1999).
[34]W. Brutting, S. Berleb, and A. G. Muckel, Synth. Met. **122**, 99 (2001).
[35]W. Brutting, S. Berleb, and A. G. Muckel, Org. Electron. **2**, 1 (2001).
[36]A. Kumar, R. Srivastava, P. Tyagi, D. S. Mehta, M. N. Kamalasanan, A. Reddy, and K. Bhanuprakash, Synth. Met. **160**, 774 (2010).
[37]H. Bassler, Phys. Status Solidi B **175**, 15 (1993).
[38]Y. Roichman, Y. Preezant, and N. Tessler, Phys. Status Solidi A **201**, 1246 (2004).
[39]B. Ries, H. Bassler, M. Grunewald, and B. Movaghar, Phys. Rev. B **37**, 5508 (1988).
[40]B. Ries and H. Bassler, Phys. Rev. B **35**, 2295 (1987).
[41]B. Movaghar, M. Grunewald, B. Ries, H. Bassler, and D. Wurtz, Phys. Rev. B **33**, 5545 (1986).
[42]S. C. Tse, H. H. Fong, and S. K. So, J. Appl. Phys. **94**, 2033 (2003).
[43]H. Park, D.-S. Shin, H.-S. Yu, and H.-B. Chae, Appl. Phys. Lett. **90**, 202103 (2007).
[44]R. G. Kepler, P. M. Beeson, S. J. Jacobs, R. A. Anderson, M. B. Sinclair, V. S. Valencia, and P. A. Cahill, Appl. Phys. Lett. **88**, 3618 (1995).
[45]K. Cho, S. W. Cho, P. E. Jeon, H. Lee, C. N. Whang, K. Jeong, S. J. Kang, and Y. Yi, Synth. Met. **158**, 984 (2008).
[46]Y. N. Gartstein and E. M. Conwell, Chem. Phys. Lett. **255**, 93 (1996).
[47]T. N. Ng, W. R. Silveira, and J. A. Marohn, Phy. Rev. Lett. **98**, 066101 (2007).

Pictiva EX2004
Samsung v Pictiva
IPR2026-00129